TECHNISCHE MECHANIK, Band 26, Heft 1, (2006), 1– 10
Manuskripteingang: 12. Oktober 2005

Bifurcations of Cylindrical Precessions of an Unbalanced Rotor

I. A. Pasynkova

The problem of stability loss of a direct synchronous cylindrical precession of an unbalanced rotor is investigated. The rigid rotor is considered as a mechanical system with four degrees of freedom. Rotation occurs at constant spin speed. Non-linear elastic bearings' reactions and viscous external and internal damping are taken into account. It is shown that different types of stability loss take place. For some range of the spin speed, jump phenomena and bi-stability occur, but the steady-state motion remains to be the direct synchronous cylindrical precession. For some other values of the parameters stability loss is accompanied by inducing hyperboloidal precession due to the conical swinging of the shaft. The precession becomes hyperboloidal as the rotor's axis traces a one-sheet hyperboloid surface. The threshold angular speed for autovibration is found. By computational modeling the limit cycles and the strange attractor are built. The results of numerical integration with slowly accelerating spin speed confirm self-centering instability under the influence of internal damping.

1 Introduction

Dynamics of an undamped rigid rotor with four degrees of freedom supported in linear elastic bearings was considered in Timoshenko, (1955) and in nonlinear bearings in Kelzon, (1992). For an ideally balanced rotor parameters of cylindrical and conical precessions were found. Dynamics of a rigid rotor with two degrees of freedom in non-linear elastic bearings with viscous external damping and linear analysis of stability one can find in Merkin, (1997). Tiwari at al. (2000) studied a 2DOF horizontal rotor taking into account the non-linearity due to radial internal clearance, Hertzian contact and varying compliance frequency. By a numerical investigation the different routes to chaos as period doubling and mechanism of intermittency were found out.

Circular whirling motion of a 4DOF unbalanced rigid rotor supported in non-linear bearings was studied in Pasynkova, (1997, 1998, 2000). A new approach to the problem was suggested. Depending on parameters of a complex amplitude the different types of precessions (cylindrical, conic or hyperboloidal) were defined. A set of non-linear resonances was found. In the case of the 2DOF unbalanced rotor supported in linear elastic bearings the set of resonances is presented by two critical frequencies. In case of non-linear elastic bearings of the Duffing's type it degenerates into a backbone curve of the dynamic response. It was shown that the type of precessions depends on the unbalance either static or dynamical. The different elastic restoring forces were considered. Only external viscous damping was taken into account. By using standard linear analysis of stability, ranges of stability loss were found. In Pasynkova, (2005) stability Loss of conic precessions of an unbalanced rigid rotor supported in non-linear elastic bearings with restoring forces of Duffing's type was investigated. External and internal linear damping were considered. Usually internal damping is taken into account for the Jeffcott rotor with flexible shaft. Not only simple linear models of internal damping were studied but non-linear (see Tondl (1974), Hagedorn at al. (1977)) and randomly varying (see Dimentberg M. (2005)) too. In case of a rigid rotor internal or "rotating" damping can be a result of rubbing between the rigid shaft and the rigid body, tightly attached to the shaft (see Dimentberg F.M., 1959; Bolotin, 1961). The similar forces can appear in the bearings with an oil film (see Bolotin, 1961; Tondl, 1974).

In this research restoring forces of Hertz's type are considered and internal viscous damping is additionally taken into account. The rotor's behavior is studied inside of instability ranges. A one-parameter bifurcation problem with the rotor angular velocity as a parameter has to be solved. When the parameter passes through the critical point in which the stability matrix has one zero-root, then methods of the elementary catastrophe theory can be applied (see Gilmore, 1981). AS it is known theoretically and practically, an influence of internal damping could be revealed in destroying of self-centering stability. Appearance of one pair of pure imaginary roots defines a threshold for inducing of autovibration, and super- or subcritical Hopf's bifurcation could take place (see Arnold,

1978; Neimark and Landa, 1987). By computational modeling it is shown that a supercritical Hopf's bifurcation occurs, and inside a narrow range of the spin speed a strange attractor could arise. Numerical integration with slowly accelerating spin speed is carried out, and divergent vibrations of the rotor are performed.

2 Basic Assumptions and Equations of Motion

A rigid rotor of mass M and length L is considered. The rotor is supported vertically in two immovable non-linear bearings at the midspan. The rotor is assumed to be dynamically symmetric with polar J_p and transversal J_t moments of inertia. The rotor is statically and dynamically unbalanced. The static eccentricity (the distance between the center of mass and the axis of revolution) is equal to e. The dynamical eccentricity is characterized by the angle δ and the phase angle ε. The angle δ is the angle between the axis of dynamical symmetry and a straight line passing through the center of mass and parallel to the axis of revolution. The angle ε is the angle between the plane passing through the axis of revolution and the center of mass and the plane containing the angle δ.

Let us assume that 1) the spin speed is constant and equal to ω; 2) rotor's displacement along the axis of revolution is negligible.

Under these assumptions the rotor can be considered as a mechanical system with four degrees of freedom.

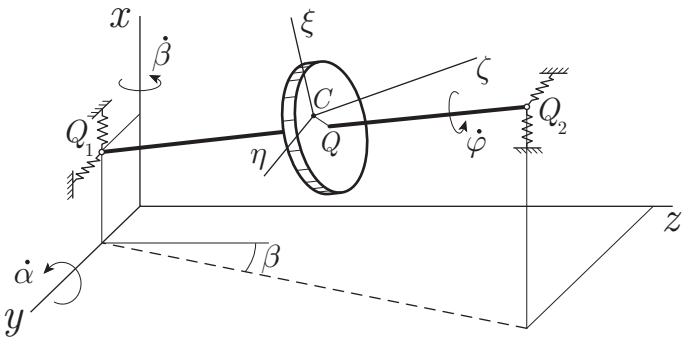

Figure 1. Rigid rotor supported in non-linear elastic bearings

Let $Oxyz$ be an inertial reference frame with the z-axis coinciding with the rotation axis of the rotor in its equilibrium state (Figure 1). One can determine Cartesian co-ordinates x_j, y_j (j=1,2) of the shaft's ends as generalized co-ordinates of the system, $S_j = x_j + iy_j$ - the displacement of the Q_j-point from the equilibrium position.

The elastic bearings are assumed to be centrally symmetric, so the reactions in the bearings only have radial components. Let the non-linear restoring forces be described by the Hertz formula $F_j = -a_0\,|S_j|^{1/2}\,S_j$.

We suggest that both external and internal damping forces are viscous and given by formulae $R_j^{(e)} = -\tilde{\mu}_e\,\dot{S}_j$, $R_j^{(i)} = -\tilde{\mu}_i\,(\dot{S}_j - i\omega\,S_j)$.

One can write non-dimensional equations of motion

$$\begin{gathered}\ddot{s}_1 + \ddot{s}_2 + (\mu_e + \mu_i)(\dot{s}_1 + \dot{s}_2) - i\,\Omega\,\mu_i(s_1 + s_2) + f_1 + f_2 = \Omega^2\exp(i\,\Omega\,\tau),\\ \ddot{s}_2 - \ddot{s}_1 + (k\,l\,(\mu_e + \mu_i) - i\,\Omega\,\lambda)(\dot{s}_2 - \dot{s}_1) - i\,\Omega\,\mu_i\,k\,l\,(s_2 - s_1) + k\,l\,(f_2 - f_1) =\\ = l\,d\,\Omega^2\exp(i\,(\Omega\,\tau - \varepsilon)),\end{gathered} \tag{1}$$

with the non-dimensional variables $s_j = S_j/(2e)$, and the non-dimensional time $\tau = \omega_0\,t$, $\omega_0 = 2\,a_0\sqrt{2e}/M$. The non-dimensional parameters are

$$\Omega = \frac{\omega}{\omega_0},\ \lambda = \frac{J_p}{J_t},\ l = 1 - \lambda,\ d = \frac{L\delta}{2\,e},\ k = \frac{M\,L^2}{4(J_t - J_p)},\ \mu_e = \frac{2\,\tilde{\mu}_e}{M\,\omega_0},\ \mu_i = \frac{2\,\mu_i}{M\,\omega_0}.$$

Non-dimensional restoring forces are $f_j = |s_j|^{1/2}\,s_j$.

3 Cylindrical Precession of Unbalanced Rotor

Firstly let us neglect damping and consider equations

$$\begin{gathered}\ddot{s}_1 + \ddot{s}_2 + f_1 + f_2 = \Omega^2 \exp(i\,\Omega\,\tau),\\ \ddot{s}_2 - \ddot{s}_1 - i\,\Omega\,\lambda\,(\dot{s}_2 - \dot{s}_1) + k\,l\,(f_2 - f_1) = l\,d\,\Omega^2 \exp(i\,(\Omega\,\tau - \varepsilon)),\end{gathered} \tag{2}$$

which admit an exact solution

$$s_j = R_j\ \exp\,(i\,\varphi_j) \exp\,(i\,\Omega\,\tau) \tag{3}$$

representing an equilibrium state in a reference frame rotating with spin speed Ω. This is a steady-state motion of the rotor. This motion is a direct synchronous precession or a circle forward whirling motion. The direct synchronous precession can be cylindrical, conic or hyperboloidal according to the surface traced in 3D space by the rotation axis. If $\varphi_1 = \varphi_2$ and $R_1 = R_2$, then (3) represents a cylindrical precession. If $\varphi_1 = \varphi_2$ or $\varphi_1 = \varphi_2 + \pi$ for $\forall R_1, R_2$, it is a conic precession, and if $\varphi_1 \neq \varphi_2$ for $\forall R_1, R_2$, it is a hyperboloidal one.

Introducing solution (3) into system (2), an inhomogeneous algebraic system with respect to the complex amplitude $R_j \exp\,(i\,\varphi_j)$ is obtained as

$$\begin{gathered}A_1\,R_1 \exp\,(i\,\varphi_1) + A_2\,R_2 \exp\,(i\,\varphi_2) = \Omega^2,\\ -B_1\,R_1 \exp\,(i\,\varphi_1) + B_2\,R_2 \exp\,(i\,\varphi_2) = d\,\Omega^2\ \exp\,(-i\,\varepsilon),\end{gathered} \tag{4}$$

with $A_j = \sqrt{R_j} - \Omega^2$, $B_j = k\,\sqrt{R_j} - \Omega^2$, $j = 1, 2$.

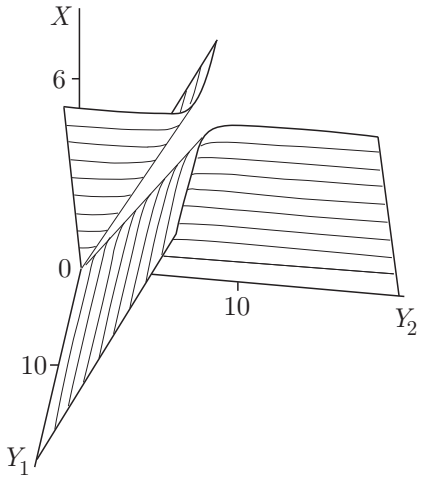

Figure 2. Set of non-linear resonances

The determinant of (4) is equal to $\Delta = A_1\,B_2 + A_2\,B_1$. The surface $\Delta = 0$ defines in the $\{R_1, R_2, \Omega^2\}$-space a set of nonlinear resonances. It is like a backbone curve in the dynamic response for Duffing's equation.
For further development it is convenient to denote $X = \Omega^2$, $Y_j = \sqrt{R_j}$. Then A_j, B_j can be rewritten as $A_j = Y_j - X$, $B_j = k\,Y_j - X$ and $\Delta = 0$ as

$$(Y_1 - X)(k\,Y_2 - X) + (Y_2 - X)(k\,Y_1 - X) = 0. \tag{5}$$

The surface of the nonlinear resonances (5) is a hyperbolic cone with a vortex point in the origin of $\{Y_1, Y_2, X\}$-space (see Figure 2). The section of this cone by the plane $X = \text{const}$ is a hyperbola. The section of the cone by the plane $Y_1 = Y_2$ is a pair of straight lines. As it was found by Pasynkova (1997), in the proximity of one part of the cone a cylindrical precession resonates, and in the proximity of the other part a conical precession resonates.

Now let us consider the statically unbalanced rotor ($e \neq 0$, $\delta = 0$). The equations (1) turn into equations

$$\begin{gathered}\ddot{s}_1 + \ddot{s}_2 + \mu_{sum}(\dot{s}_1 + \dot{s}_2) - i\,\Omega\,\mu_i(s_1 + s_2) + f_1 + f_2 = \Omega^2 \exp(i\,\Omega\,\tau),\\ \ddot{s}_2 - \ddot{s}_1 + (k\,l\,\mu_{sum} - i\,\Omega\,\lambda)(\dot{s}_2 - \dot{s}_1) - i\,\Omega\,\mu_i\,k\,l\,(s_2 - s_1) + k\,l\,(f_2 - f_1) = 0,\end{gathered} \tag{6}$$

with $\mu_{sum} = \mu_e + \mu_i$. The system (6) also admits the exact solution in the form (3), and the corresponding algebraic equations are

$$\begin{gathered}(A_1 + i\,\mu_e\,\sqrt{X})\,Y_1^2 \exp\,(i\,\varphi_1) + (A_2 + i,\mu_e\,\sqrt{X})\,Y_2^2 \exp\,(i\,\varphi_2) = X,\\ -(B_1 + i\,k\,\mu_e\,\sqrt{X})\,Y_1^2 \exp\,(i\,\varphi_1) + (B_2 + i\,k\,\mu_e\,\sqrt{X})\,Y_2^2 \exp\,(i\,\varphi_2) = 0.\end{gathered} \tag{7}$$

The system (7) can be considered with respect to $\exp\,(i\,\varphi_j)$ and the solution can be written as

$$\exp\,(i\,\varphi_j) = \frac{X(B_{3-j} + i\,k\,\mu_e\,\sqrt{X})}{Y_j^2\,\Delta_\mu}, \tag{8}$$

where $\Delta_\mu = \Delta - 2\,k\,\mu_e^2\,X + i\,\mu_e\,\sqrt{X} \sum\limits_{j=1,2} (k\,A_j + B_j) \neq 0$.

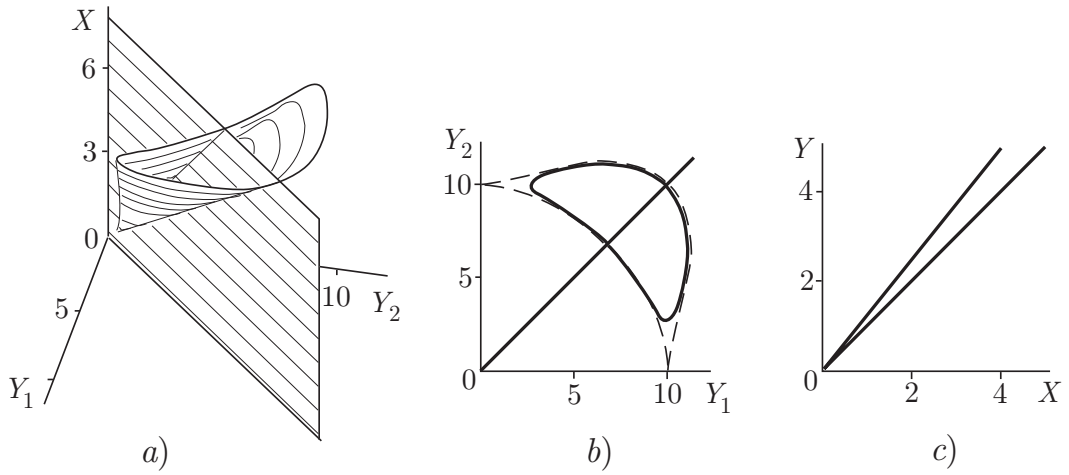

Figure 3. Surface of localization of equilibrium states

By using the property $|\exp(i(\varphi_1 - \varphi_2))| = 1$ one can find out that in the $\{X, Y_1, Y_2\}$-space equilibrium states are located on the surface

$$\begin{gathered}(Y_1 - Y_2)[L_2\, L_3 - \mu_e^2\, k^2\, X\, (Y_1 + Y_2)(Y_1^2 + Y_2^2)] = 0,\\ L_2 = k(Y_1^2 + Y_1\, Y_2 + Y_2^2) - X(Y_1 + Y_2), \quad L_3 = k(Y_1^3 + Y_2^3) - X(Y_1^2 + Y_2^2),\end{gathered} \tag{9}$$

which consists of the plane $Y_1 = Y_2$ and the cone with vortex point in the origin.

3D-plot of surface (9) and its sections by planes $X = \mathrm{const}$ and $Y_1 = Y_2$ are shown on Figure 3 for parameters $X = 8$, $k = 0.8$, $\mu_e = 0.18$,(the thick line) and $\mu_e = 0$ (the dashed line).

Let us study equilibrium states located on the plane $Y_1 = Y_2$. From relation (8) it follows that $\exp(i\,\varphi_1) = \exp(i\,\varphi_1)$ and $\varphi_1 = \varphi_1 = \varphi$. The corresponding whirling motion is the cylindrical precession, and the non-dimensional displacement in the complex form is given by formula

$$s = R\, \exp(i\,\varphi)\, \exp(i\,\Omega\,\tau), \tag{10}$$

where $R = Y^2$, $\exp(i\,\varphi) = X(B + i\,k\,\mu_e\,\sqrt{X})/Y^2\,\Delta_\mu$, $A = Y - X$, $B = k\,Y - X$, $\Delta_\mu = 2\,(A\,B - k\,\mu_e^2\,X + i\,\mu_e\,\sqrt{X}(k\,A + B))$.

From the property $|\exp(i\,\varphi)| = 1$, the dynamic and phase responses of the cylindrical precession can be computed as

$$Y^2\,\sqrt{A^2 + \mu_e^2\,X} = \frac{X}{2}, \qquad \tan\varphi = -\frac{\mu_e\,\sqrt{X}}{A}. \tag{11}$$

As it follows from (11), self-centering takes place and the limit value Y_∞ under $X \to \infty$ can be computed as $Y_\infty = \lim_{X\to\infty} Y(X) = 1/\sqrt{2} \approx 0.707$.

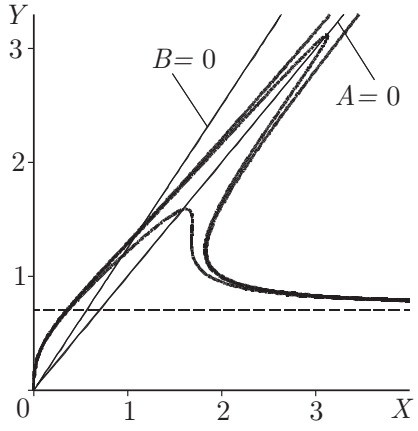

Figure 4. Dynamic responses and non-linear resonances

In Figure 4 the dynamic responses for three different values of the external damping coefficient $\mu_e = 0$ (unclosed curve), $\mu_e = 0.09$, $\mu_e = 0.25$ are shown with thick lines. The resonances $A = 0$ and $B = 0$ are shown with thin lines. The line $Y = Y_\infty$ is shown by a dashed one.

The dynamic response for the 2DOF rotor is given by the same formula (11) because the second equation in (6) is satisfied identically for the solution $s_1 = s_2$ (see Merkin, 1997). But in case of the 2DOF model there is only one non-linear resonance $A = 0$, and the other $B = 0$ could not be revealed.

One can note that the dynamic response, the set of non-linear resonances and other characteristics do not depend on the coefficient of internal damping μ_i.

To investigate stability of the cylindrical precession one can apply standard linear analysis. A linear approximation of the perturbation system corresponding to (6), which is of the differential order eight, falls into two independent sub-systems each of which is of fourth order. Therefore, the characteristic polynomial also splits up into two polynomials of fourth order. We denote these polynomials as $P_j, (j = 1, 2)$ and its coefficients as $a_q^{(j)}$, $q = \overline{0, 4}$. Applying a usual procedure, the coefficients $a_q^{(2)}$ can be computed as

$$a_0^{(2)} = 1, \quad a_1^{(2)} = 2\,k\,l\,\mu_{\rm sum}, \quad a_2^{(2)} = \frac{5}{2}\,k\,l\,Y + (1 + l^2)\,X + k^2\,l^2\,\mu_{\rm sum}^2,$$
$$a_3^{(2)} = kl(\frac{5}{2}k\,l\,\mu_{\rm sum}Y + 2(\mu_e - l\,\mu_i)X),\; a_4^{(2)} = l^2((kY - X)(\frac{3}{2}kY - X) + k^2\mu_e^2 X). \tag{12}$$

Imposing $k = 1$, $l = 1$, the coefficients $a_q^{(1)}$ can be obtained from formulae (12).

The first three coefficients of each polynomial P_j are always positive $a_q^{(j)} > 0, q = \overline{0, 2}$. It can be easy checked that the two first Hurwitz's determinants are positive, too. If internal damping is significant, then the coefficients $a_3^{(j)}$ could become negative for sufficiently big values of X and limited values of Y, but $a_4^{(j)} > 0$. This fact indicates that self-centering regimes can not be stable. Moreover, if $a_3^{(j)} < 0$ and $a_4^{(j)} > 0$, the Hurwitz's determinant of third order

$$\Delta_3(P_j) = -a_0^{(j)}\,(a_3^{(j)})^2 - a_4^{(j)}\,(a_1^{(j)})^2 + a_1^{(j)}\,a_2^{(j)}\,a_3^{(j)} < 0, \tag{13}$$

and self-centering regimes for large values of X are unstable. This confirms the well-known fact that internal damping can destroy self-centering stability.

4 Bifurcations of Cylindrical Precession

Now let us study conditions of stability loss of the cylindrical precessions. As we consider $X = \Omega^2$ as a parameter, we encounter a one-parameter problem of bifurcation. Curves $a_4^{(j)} = 0, (j = 1, 2)$ define a set of bifurcation on the $\{X, Y\}$-plane and the points of intersection of the dynamic response with these curves are critical or degenerated ones. For parameters $k = 0.8$, $\mu_e = 0.09$, $\lambda = 0.7$ the dynamic response is shown on Figure 5. The critical points are numerated as $I - IV$. Their coordinates are $(X_1 = 1,1358,\, Y_I = 1.4064)$, $(X_{II} = 1.8187,\, Y_{II} = 1.2291)$, $(X_{III} = 2.0290,\, Y_{III} = 1.7040)$, $(X_{IV} = 3.1477,\, Y_{IV} = 3.1312)$.

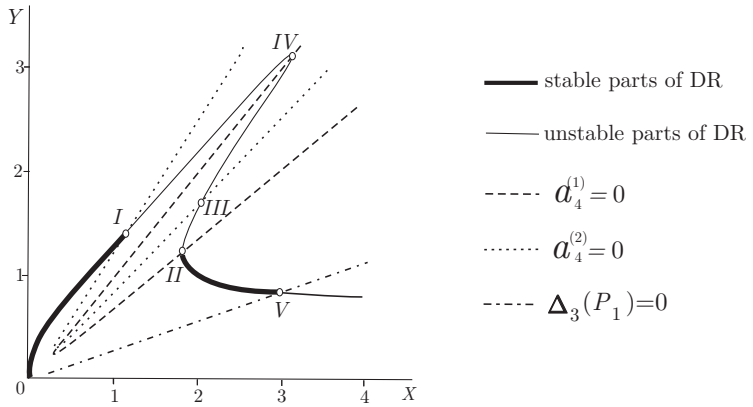

Figure 5. The dynamic response (DR) of cylindrical precession

In the reference frame rotating with the spin speed Ω the equations of motion are autonomous, and one can apply elementary catastrophe theory. As we consider a one-parameter problem, there is the simplest type of catastrophe. According to a theory when the parameter passes through its critical value, the degenerated point can split up to three non-degenerated points, and their localization and stability properties can be changed (see Gilmore, 1981). By studying the intersection of the curves $|\exp(i(\varphi_1 - \varphi_2))| = 1$ (in Figure 6 it is shown by thick line) and $|\exp(i\,\varphi_1)| = 1$ (in Figure 6 it is shown by thin line) on the plane $X = \text{const}$, one can observe bifurcations of cylindrical precession.

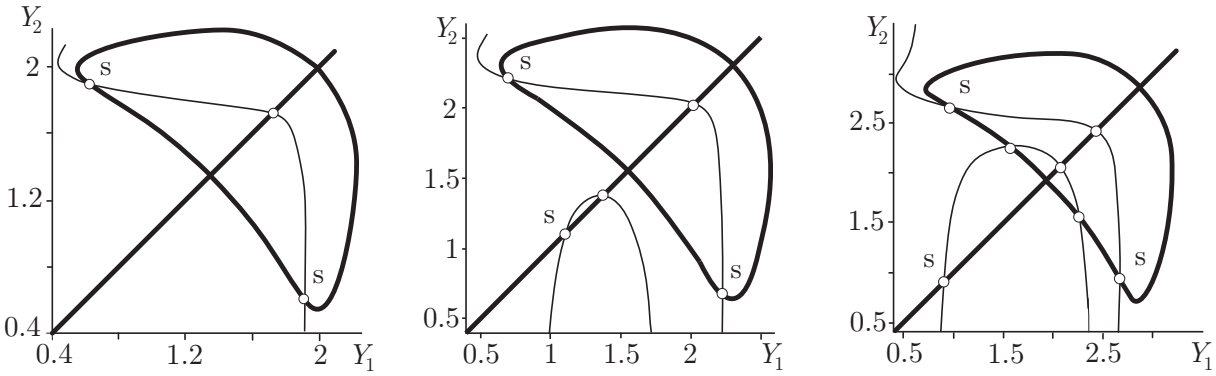

a) X = 1.4; b) X = 1.9; c) X = 2.4;

Figure 6. Bifurcations of cylindrical precession when parameter X passes through the degenerated points

When parameter X approaches the first critical value (point I), the cylindrical precession becomes unstable and two other stable precessions appear, but they are of the hyperboloidal type. On the plane $X = \text{const}$ one can see three points of intersection, one of them is located on the bisectrix and corresponds to an unstable whirling motion, two others are located on the cone's surface (9) and parameterize stable non-symmetrical ($Y_1 \neq Y_2$) hyperboloidal precessions (see Figure 6, a). Further, when X passes through the second critical point (point II), one can observe a jump phenomenon, as two more points of intersection appear on the bisectrix on the plane $X = \text{const}$ (see Figure 6, b). Also the point III splits up to three non-critical points (see Figure 6, c). At last, when X passes through the fourth critical point (point IV), three non-critical points merge into one point located on the low branch of the dynamic response (see Figure 5).

Note that in case of 2DOF only instability in the proximity of the resonance $A = 0$ can be observed. In other words, only jump phenomena can be found. Stability loss with simultaneous changing of the motion type can not be revealed.

5 Supercritical Hopf's Bifurcation, Limit Cycles and Strange Attractors

Now let us consider bifurcations when parameter X passes through the critical point V (Figure 5), in which the matrix of stability has one pair of pure imaginary roots. By the theory (see Arnold, 1978; Gilmore, 1981; Neimark and Landa, 1987) one of two types of bifurcation could take place: super- or subcritical Hopf's bifurcation or in Russian terminology, soft or hard character of bifurcation. In the first case instability loss occurs with simultaneous detachment of a stable limit cycle. In the second case merging with an unstable limit cycle happens. Numerical computation reveals the supercritical Hopf's bifurcation in case of a dynamically prolated rigid rotor. Stable limit cycles of the cylindrical type exist for $\forall X > X_V$, and the average amplitude of the precession increases when X increases. The value X_V gives a threshold of autovibration excitation. Numerical solving of the equations

$$Y^2\sqrt{A(X,Y)+\mu_e^2 X} = X/2, \quad \Delta_3(P_1) = 0 \tag{14}$$

for a wide range of μ_e reveals that X_V only depends on the ratio $\chi = \mu_i/\mu_e$.

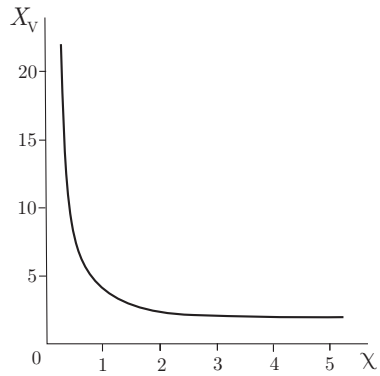

Figure 7. Threshold of autovibration excitation as a function of the ratio $\chi = \mu_i/\mu_e$

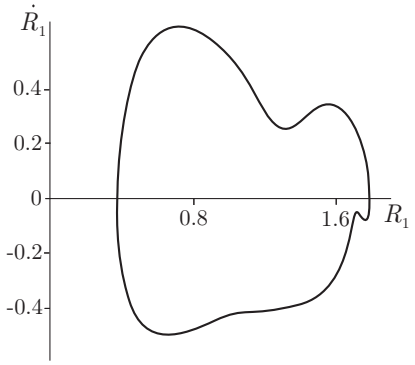

Figure 8. Limit cycle for $X = 3.15$

This result is presented in the Figure 7. One can conclude that if $\chi < 1$, even a small decreasing of internal damping can move away the threshold of autovibration excitation.

For the parameters $k = 0.8$, $\lambda = 0.7$, $\mu_e = 0.09$, $\mu_i = 0.13$ the limit cycle in the plane $\{R_1, \dot{R}_1\}$ for $X = 3.15$ is shown in Figure 8. The limit cycle in the plane $\{R_2, \dot{R}_2\}$ is the same one, the equality of the phases $\varphi_1 = \varphi_2$ confirms that the precession is cylindrical.

The cylindrical limit cycles becomes sensitive to initial conditions in a narrow range of X close to the critical point V with $X_V = 2.986$. This range extends to $X = 3.2$. If the initial values are $R_1 \neq R_2$ or $\varphi_1 \neq \varphi_2$, then the cylindrical limit cycle turns out to be unstable. And a typical process seems to pass in the following manner: after some revolutions quite close to Hopf's limit cycle, a double-loop limit cycle appears and period doubling occurs. Then the double-loop limit cycle slips into chaotic motion and we can observe a strange attractor. After a certain period of time the motion is synchronized and a new type of limit cycle becomes settled (as a rule with double loop).

Below the results of a numerical integration of equations (2) are presented. The typical process can be seen for $X = 3.15$. In the $\{R_1, \dot{R}_1\}$-plane of 6-space $\{R_1,\ \dot{R}_1,\ R_2,\ \dot{R}_2,\ \varphi_1 - \varphi_2,\ \dot{\varphi}_1 - \dot{\varphi}_2,\}$ a phase portrait for 700 revolutions of the rotor is plotted (see Figure 9).

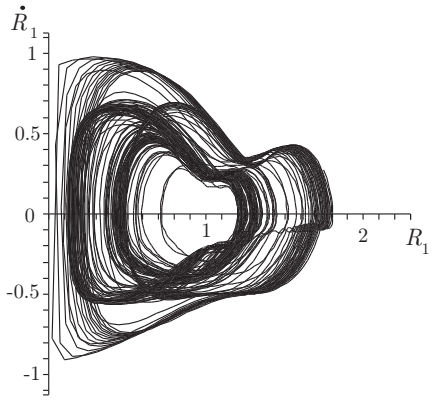

Figure 9. Phase trajectory for 700 revolutions of the rotor

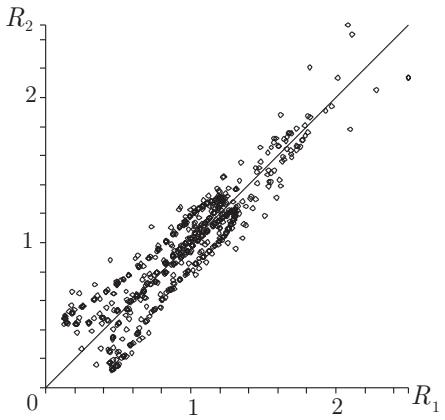

Figure 10. Poincaré's map

In Figure 10 the Poincaré section is plotted in the plane $\{R_1, R_2\}$ ($\tau = \mathrm{mod}(2\,\pi/\Omega)$), and confirms the existence of a transient strange attractor. One can see a distinct contour of the synchronized motion.

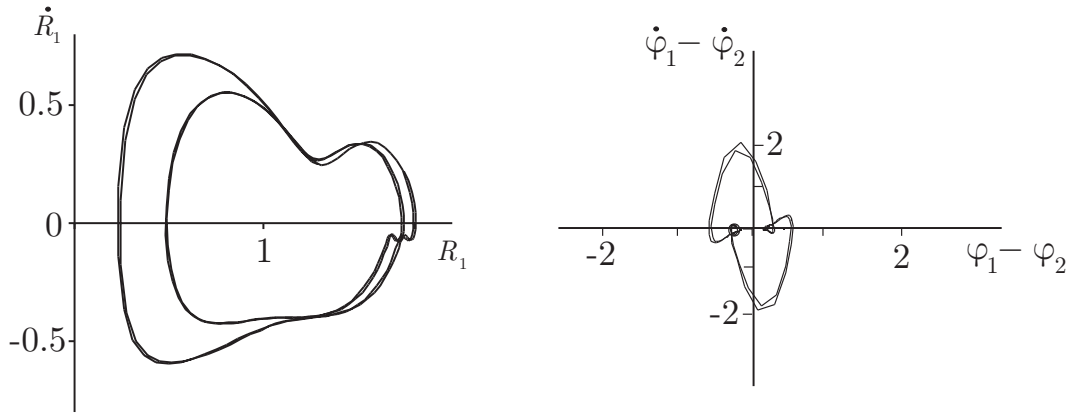

Figure 11. Phase trajectories from 30 to 50 revolutions of the rotor

The phase trajectories in the $\{R_1, \dot{R}_1\}$-plane and in the $\{\varphi_1 - \varphi_2,\ \dot{\varphi}_1 - \dot{\varphi}_2\}$-plane at the beginning of motion and at the end of it are presented in Figures 11, 12.

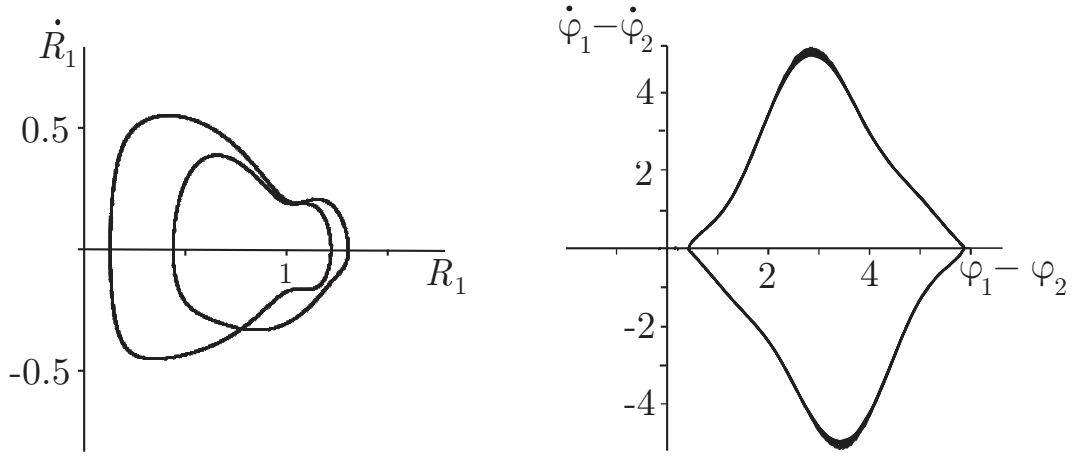

Figure 12. Phase trajectories from 600 to 700 revolutions of the rotor

One can see that in the beginning the precession is close to a cylindrical one because the phase angles difference $|\varphi_1 - \varphi_2|$ is sufficiently small (see Figure 11), but then a conic swinging of the axis of revolution increases, the difference $|\varphi_1 - \varphi_2|$ becomes large (see Figure 12), and the motion turns out to be hyperboloidal.

6 Acceleration of a Statically Unbalanced Rotor

Now let us assume that the spin speed accelerates under the law

$$\Omega = \Omega_0 + \nu\,\tau. \tag{15}$$

By taking into account the angular acceleration ν, the equations of motion (6) can be modified (see Genta, 1999)

$$\begin{aligned} &\ddot{s}_1 + \ddot{s}_2 + \mu_{sum}(\dot{s}_1 + \dot{s}_2) - i\,\Omega\,\mu_i(s_1 + s_2) + f_1 + f_2 = (\Omega^2 - i\,\nu)\exp(i\,(\Omega\,\tau + \nu\,\tau^2/2)),\\ &\ddot{s}_2 - \ddot{s}_1 + (k\,l\,\mu_{sum} - i\,\Omega\,\lambda)(\dot{s}_2 - \dot{s}_1) - i\,\Omega\,(\mu_i\,k\,l + \nu\,\lambda)(s_2 - s_1) + k\,l\,(f_2 - f_1) = 0, \end{aligned} \tag{16}$$

Results of a numerical integration of equations (16) for the same values of parameters k, λ, μ_e, μ_i are presented in Figure 13 for $\nu = 0.005$ (see Figure 13,a) and $\nu = 0.02$ (see Figure 13,b).

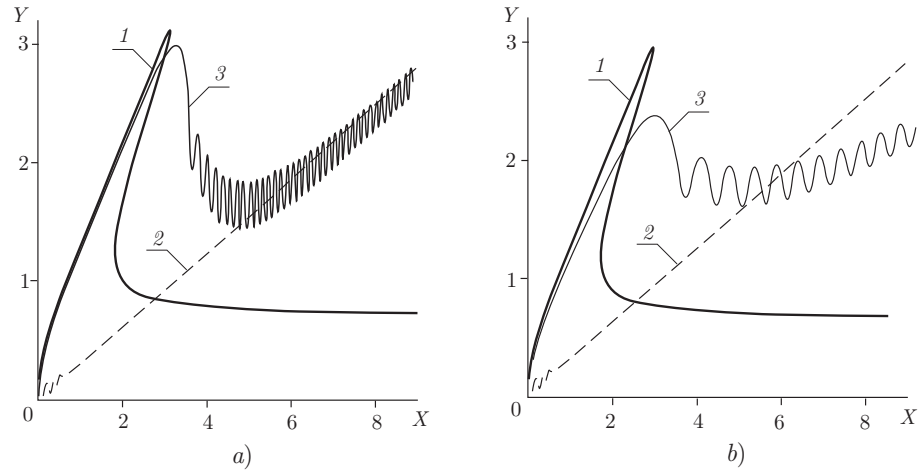

Figure 13. The dynamic response of the cylindrical precession (curve 1), the bifurcation set $\Delta_3\,(P_1) = 0$ (curve 2) and acceleration of the unbalanced rotor through the critical speeds (curve 3), initial values $R_1(0) = R_2(0)$

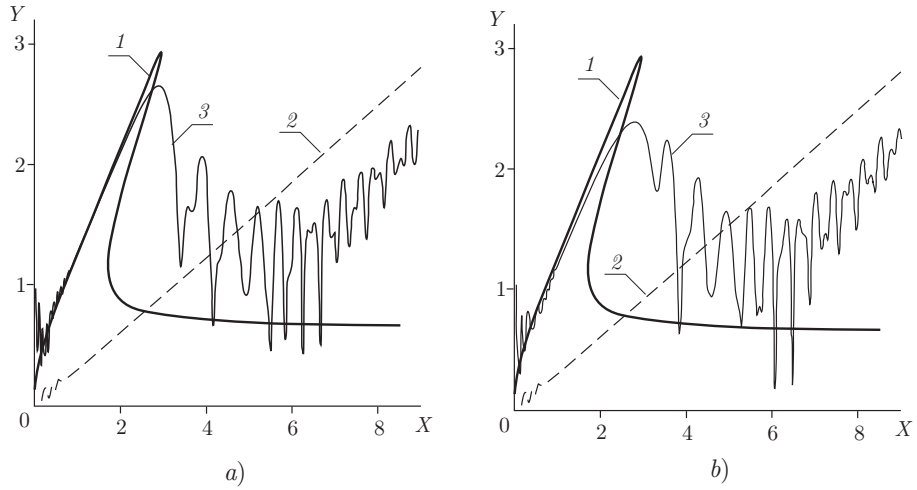

Figure 14. The dynamic response of the cylindrical precession (curve 1), the bifurcation set $\Delta_3(P_1) = 0$ (curve 2) and acceleration of the unbalanced rotor through the critical speeds (curve 3), initial values $R_1(0) \neq R_2(0)$

The non-stationary crossing of the resonance zone is sensitive to the initial conditions. The motions, shown in Figure 13, are cylindrical. The conic swinging of the revolution axis does not occur. If the initial conditions for the bearing 1 are not equal to the corresponding values for the bearing 2, the non-stationary crossing of the resonance zone results in a complex hyperboloidal type. In Figure 14, a) and b) the time processes for Y_1 and Y_2 are shown correspondingly.

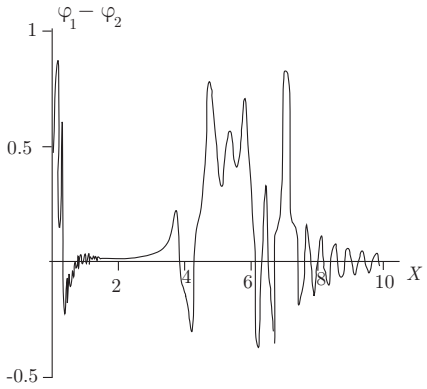

Figure 15. The time process for the phase difference $(\varphi_1 - \varphi_2)$. Initial values $R_1(0) \neq R_2(0)$

In Figure 15 the time process for the phase difference $(\varphi_1 - \varphi_2)$ is plotted. One can see that oscillations after the "jump" of amplitude are chaotic.

7 Conclusions

Introduction of a 4DOF model of an unbalanced rigid rotor allows studying a complex three-dimensional whirling motion, which is described by a coupled differential equations of eighth order and presented by cylindrical, conic or hyperboloidal precession.

The suggested approach allows to consider the different types of non-linearities, with or without a linear component, and obtain the dynamic response of the whirling motion for all values of an angular velocity.

This problem definition reveals some effects that could not be found for a 2DOF model, such as instability with simultaneous changing of the motion type, etc. It becomes possible to study an influence not only a static unbalance, which is usual, but also a dynamical unbalance simultaneously.

References

Arkhipova I. M., Pasynkova I. A.: Investigation of Precessions of an Unbalanced Rotor. *The 2nd Polyakhov Readings: The Selected Proceeding*. Saint-Petersburg, 2000, 65-72 (in Russian).

Arnold V. I.: *Theory of Differential Equations: Additional Chapters*. Moscow, Nauka, 1978 (in Russian).

Bolotin V. V.: *Nonconservative Problems of the Theory of Elastic Stability*, Pergamon Press, New York, 1963. (Fizmatgiz Publisher, Moscow, 1961 (in Russian)).

Genta G.: *Vibration of structures and machines: practical aspects* 3rd ed. New York, Springer, 1999.

Gilmore R.: *Catastrophe theory for scientists and engineers*. New Jork, John Wiley & Sons, 1981.

Dimentberg F. M.: *Flexural Vibrations of Rotating Shafts*. Butterworth, London, 1961.

Dimentberg M. F.: Vibration of a rotating shaft with randomly varying internal damping. *Journal of Sound and Vibration* (2005) **285**, 759-765.

Hagedorn P., Kühl H., Teshner W.: Zur Stabilität einfach besetzer Wellen mit nichtlinearer innerer Dämpfung. *Ingenieur-Archiv*, **46**, 1977, 203-212.

Kelzon A. S., Meller A. S.: On the Dynamics of Rotors Supported in Ball Bearings. *Doklady RAS*, v.323, N5, 1992, 851-857 (in Russian).

Merkin D. R.: *Introduction to the Theory of Stability*. New York, Springer, 1997.

Neimark Yu. I., Landa P. S.: *Stochastic and Chaotic Oscillations*. Dordrecht, Boston, Kluwer Academic. Publishers, 1992. (Moscow, Nauka, 1987 (in Russian)).

Pasynkova I. A.: Hyperboloidal Precession of Rotor in Nonlinear Elastic Bearings. *Vestnik of St.-Petersburg University*, p.I, 4, 1997, 88-95 (in Russian).

Pasynkova I. A.: Stability of Rigid Unbalanced Rotor Conic Precession. *Vestnik of St.-Petersburg University*, p.I, 1, 1998, 82-86 (in Russian).

Pasynkova I. A.: Stability Loss of Conic Precessions of an Unbalanced Rotor in Quasilinear Elastic Bearings. *Vestnik of St.-Petersburg University*, p.I, 2, 2005, 118-125 (in Russian).

Timoshenko S. P.: *Vibration Problems in Engineering*. Toronto, Van Nostrand, 1955.

Tiwari M., Gupta K., Prakash O.: Dynamic response of an unbalanced rotor supported in ball bearings *Journal of Sound and Vibration* (2000) **238**(5), 757-779.

Tondl A.: Problems of Self-Excited Vibrations of Rotors. *Monographs and Memoranda Series*, #17, SVUSS, Bechovice, Czechoslovakia, 1974.

Address: Dr. Inna A. Pasynkova, Saint-Petersburg State University, Faculty of Mathematics and Mechanics, Universitetsky pr. 28, Stary Peterhof, 198504, St. Petersburg.
email: ip@ip1157.spb.edu